# Exhibit IND9

NIH Public Access
Author Manuscript
*Neuroimage*. Author manuscript; available in PMC 2007 March 7.

Published in final edited form as:
*Neuroimage*. 2007 January 15; 34(2): 733–742.

# Diffusion Tensor Imaging in Children and Adolescents: Reproducibility, Hemispheric, and Age-Related Differences

**David Bonekamp**[1], **Lidia M. Nagae**[1,2], **Mahaveer Degaonkar**[1,2], **Melissa Matson**[2,3], **Wael M. A. Abdalla**[1], **Peter B. Barker**[1,2], **Susumu Mori**[1,2], and **Alena Horská**[1]

1 *The Russell H. Morgan Department of Radiology and Radiological Science, Johns Hopkins University, Baltimore, Maryland, United States*

2 *FM Kirby Research Center for Functional Brain Imaging, Kennedy Krieger Institute, Baltimore, Maryland, United States,*

3 *Department of Psychiatry and Behavioral Sciences, Johns Hopkins University School of Medicine, Baltimore, Maryland, United States*

## Abstract

We evaluated intra-rater, inter-rater, and between-scan reproducibility, hemispheric differences, and the effect of age on apparent diffusion coefficient (ADC) and fractional anisotropy (FA) in healthy children (age range 5.5–19.1 years) examined with a clinical diffusion tensor imaging (DTI) protocol at 1.5 T, using a region of interest (ROI) methodology. Measures of reliability and precision were assessed in six ROIs using two different ROI shapes (polygonal and ellipsoidal).

RESULTS: Highly reproducible values of ADC and FA were obtained with the polygonal method on intra-rater (coefficients of variation ≤ 2.7%) and inter-rater (coefficients of variation ≤ 4.8%) reproducibility. For between scan reproducibility, the coefficients of variation were ≤ 9.5%. Mean asymmetry indices were in the range from −4% to 9% for FA and from −6% to 3% for ADC. ADC showed significant negative correlation with age in 13 of 15 examined fiber tracts and FA increased significantly in three fiber tracts. Our results show that the evaluated DTI protocol is suitable for clinical application in pediatric population.

### Keywords

Diffusion tensor imaging; fractional anisotropy; apparent diffusion coefficient; reproducibility; hemispheric differences; brain maturation; children

## INTRODUCTION

Diffusion tensor imaging (DTI) (Basser, *et al.*, 1994) provides a unique tool to non-invasively visualize and quantitatively characterize brain white matter pathways both in healthy brains (Wakana, *et al.*, 2004) and under pathological conditions. For example, prior studies have demonstrated the ability of DTI to identify white and gray matter abnormalities in schizophrenia (Sun, *et al.*, 2003), epilepsy (Briellmann, *et al.*, 2003) and multiple sclerosis (Cassol, *et al.*, 2004), reflecting microstructural changes underlying the disease processes.

**Corresponding author:** Alena Horská, Ph.D., The Russell H. Morgan Department of Radiology and Radiological Science, Johns Hopkins University, 217 Traylor Bldg. 720 Rutland Ave. Baltimore, MD 21205, Phone: (410) 614-2707, FAX: (410) 614-1948, E-mail: ahorska@jhmi.edu.

NIH-PA Author Manuscript
NIH-PA Author Manuscript
NIH-PA Author Manuscript

NIH-PA Author Manuscript NIH-PA Author Manuscript NIH-PA Author Manuscript

Since DTI is becoming part of many standard clinical MRI protocols, the availability of normative data is essential for interpretation of pathological findings. DTI has been applied by several groups to investigate white matter development in infants and children (Hermoye, *et al.*, 2006; Jones, *et al.*, 2003; McGraw, *et al.*, 2002; Miller, *et al.*, 2003; Mukherjee, *et al.*, 2001). For this age group, reference data on age-related differences in apparent diffusion coefficient (ADC) and fractional anisotropy (FA) in major fiber tracts recently became available (Hermoye, *et al.*, 2006). However, there are very few normative DTI data for children and adolescents. Two previous studies evaluated children in a narrow age range (8–12 years old) (Klingberg, *et al.*, 1999; Snook, *et al.*, 2005). Voxel-wise analyses were used in two studies with a larger number of subjects and a wider age interval (5–18 years, (Schmithorst, *et al.*, 2002) and 6–19 years, (Barnea-Goraly, *et al.*, 2005)) to examine age-related differences in ADC and FA. Schmithorst et al. (Schmithorst, *et al.*, 2002) reported a negative correlation between the trace of the ADC and age throughout the white matter and an increase in FA with age in four fiber tracts (internal capsule, corticospinal tract, left arcuate fasciculus, and right inferior longitudinal fasciculus) while Barnea-Goraly et al (Barnea-Goraly, *et al.*, 2005) found more widespread age-related differences in FA in children and adolescents. While voxelwise methods employed in both papers (Barnea-Goraly, *et al.*, 2005; Schmithorst, *et al.*, 2002) can be used for analyses of the entire brain, they require inter-subject registration and image smoothing, and comprise a large number of statistical tests that may increase Type I errors. In our analyses, we therefore used a region-of-interest (ROI) based approach similar to that employed in a recent DTI study of early brain development (Hermoye, *et al.*, 2006) to assess age-related and hemispheric differences in ADC and FA in 15 selected white matter tracts in healthy children and adolescents.

For follow-up of longitudinal DTI studies, knowledge of measurement reproducibility in ADC and FA is essential in order to predict detectable changes. However, data on reproducibility are limited (Ciccarelli, *et al.*, 2003; Pfefferbaum, *et al.*, 2003) and no quantitative evaluation of regional differences in ADC and FA reproducibility is available in the literature. Our main goal therefore was to establish reproducibility in pediatric DTI data. We evaluated intra-rater, inter-rater, and between-scan reproducibility of ADC and FA measurements, using two different ROI drawing methods. To our knowledge, this is the first study to evaluate in detail ADC and FA reproducibility, hemispheric differences, and the effect of age in healthy, thoroughly screened children and adolescents using a typical, clinical DTI protocol on a standard 1.5T scanner.

## MATERIAL AND METHODS

Typically developing children ages 5–18 years were recruited from the Baltimore, MD area by advertisement. Each participant and parent signed a consent form that met the institutional review board standards of the Johns Hopkins Medical Institutions. Participants were initially screened over the telephone and excluded if there was a history of neurological disorder, mental retardation, or learning disability. Parents of those children meeting these eligibility criteria participated in a structured diagnostic interview using the Diagnostic Interview for Children and Adolescents – Fourth Edition (DICA-IV; (Reich, et al., 1997; Welner, et al., 1987)), which is based on the Diagnostic and Statistical Manual of Mental Disorders – Fourth Edition (DSM-IV). Children meeting DSM-IV criteria for a psychiatric disorder were subsequently excluded.

Forty children (22 boys, mean age 13.7±3.5 years, age range 5.5 – 19.1 years) were included. For intra-rater and inter-rater reproducibility we evaluated data from the first ten subjects (3 boys, mean age 14.3±2.8 years, age range 10–18.5 years) who successfully completed the 45 minute MRI protocol (Bonekamp, *et al.*, 2005). To evaluate between-scan reproducibility, we examined 10 participants (7 boys, mean age 14.1±2.8 years, age range 8.8–18.0 years) who completed the MRI protocol and agreed to undergo another scan either on the same day, or

NIH-PA Author Manuscript NIH-PA Author Manuscript NIH-PA Author Manuscript

who could return for a follow-up scan within 6 weeks of the initial scan (the mean time between scans was 15.3±16.7 days, with 4 examinations being performed on the same day as the initial). Four of the individuals included in this part of the study also participated in the intra- and inter-rater reproducibility part of the protocol.

Magnetic resonance imaging was performed using a 1.5-T scanner (General Electric Medical Systems, Waukesha, WI) equipped with 40-mT/m gradients. The examination was performed with the patient in the supine position with the standard circularly polarized birdcage transmit-receive head coil. The DTI sequence (4:48 minutes scan time) was the last series in a 45 minutes long MR protocol including conventional MRI and proton MR spectroscopic imaging (data not reported here). DTI data were acquired using a single-shot diffusion-weighted spin-echo echo-planar imaging sequence with the following parameters: TE=93.7 ms, acquisition matrix 96×96, field-of-view 240 mm, two b=0 s/mm$^2$ images, 15 diffusion-weighted images applied in different directions (Jones, *et al.*, 1999), maximum b=1000 s/mm$^2$, 2 acquisitions, 24 axial slices parallel to the anterior commissure - posterior commissure plane, 5 mm slice thickness, no gap. One slice contained both the anterior and the posterior commissures. The position and orientation of the DTI slices on a mid-sagittal image was used to prescribe the slice position and orientation for the follow-up examination.

Diffusion tensors were computed using the method of Basser et al. (Basser, *et al.*, 1994) with DTI Studio (H. Jiang and S. Mori, Johns Hopkins University, cmrm.med.jhmi.edu) and DTIPROC (C. K. Jones, Johns Hopkins University). Individual images were visually inspected for motion artifacts, and discarded if necessary. Voxel-wise multivariate linear least squares fitting of the intensity of the multiple diffusion-weighted images and diagonalization of the diffusion tensor was performed to obtain the six elements of the symmetric diffusion tensor (Basser and Pierpaoli, 1998) and the ADC and FA values (Basser, *et al.*, 1994).

The parametric ADC, FA, and color coded image maps (Pajevic and Pierpaoli, 1999) were transferred to an IBM PC compatible computer and ROIs drawn using DSXJHMI (P. B. Barker and D. Bonekamp, Johns Hopkins University, godzilla.kennedykrieger.org). ROI drawing was performed on the color-coded maps, using the color information and intensity to identify fiber bundles and avoid gray matter (the color maps are modulated by the FA images to suppress signal from gray matter).

Fifteen regions of interest were evaluated in all subjects (Figure 1): cerebral peduncle (1), temporal white matter (2), frontal white matter (3), anterior limb of the internal capsule (4), posterior limb of the internal capsule (5), genu (6), splenium (7), body of the corpus callosum (8), anterior white matter (9), temporo-occipital white matter (10), superior longitudinal fasciculus (11), superior corona radiata (12), superior fronto-occipital fasciculus (13), cingulum (14), centrum semiovale (15). For the analysis of ADC and FA reproducibility, six different fiber bundles were selected: cerebral peduncle, anterior limb and posterior limb of internal capsule, genu of the corpus callosum, superior corona radiata, and cingulum (Figure 2). All measurements were performed in both hemispheres, at a fixed level for each structure.

The selection of the slice in which the cerebral peduncle was outlined was made by choosing the first slice above the decussation of the superior cerebellar peduncle. The superior corona radiata was outlined in the most rostral slice that still clearly showed the radiation of the callosal fibers. A full cross-section of the superior part of the cingulum was usually only seen in one slice and easily identified. The ROIs for the genu of the corpus callosum, the anterior limb and posterior limb of the internal capsule were all placed in the same slice. Criteria for selection of this slice were a broad cross section of the basal ganglia, visibility of a middle cross-section of the genu and splenium of the corpus callosum, and the broadest diameter of the internal capsule when compared to adjacent slices. Using this approach, one single slice meeting all

NIH-PA Author Manuscript NIH-PA Author Manuscript NIH-PA Author Manuscript

criteria could usually be identified. The ROIs were drawn with two different techniques in all regions – polygonal and ellipsoid ROIs. Each polygonal ROI was drawn to encompass the largest portion of the fiber tract cross-section that was clearly identifiable, and avoid any signal drop off into the background. Ellipsoid ROIs were placed along the long axis of the particular fiber tract in one slice, spaced so as to sample different regions of the tract. The size of the ellipsoid ROIs was chosen to encompass 16 pixels (from interpolated data to a 256×256 matrix), and the number of ellipsoid ROIs to be placed on one single fiber tract cross-section was predefined for each ROI on a template given to all operators (number of ellipsoid ROIs: cerebral peduncle (2), anterior limb of the internal capsule (3), posterior limb of the internal capsule (3), genu of the corpus callosum (2), superior corona radiata (5); cingulum (5)). ROIs were drawn five times by one rater (D.B.) (with evaluations separated by 1 to 3 days) to evaluate the intra-rater reproducibility of the method, and one time by four raters (D.B., L. M. N.-P., M.D., M.M.) for inter-rater reproducibility analysis. All raters were given a template (corresponding to Figure 2) and performed their evaluations independently. ROIs for the between-scan reproducibility were drawn by one rater (D.B.).

All ROIs were transferred to a Linux workstation and overlaid on ADC maps and FA maps and an average b=0 $mm^2/s$ image, using DSXJHMI software. The intensity values from all voxels in one ROI were averaged. Voxels with image intensity in the range of cerebrospinal fluid (CSF) on the b=0 $mm^2/s$ image (as determined from the minimum value found in the lateral ventricles) were excluded, as were voxel locations with FA values lower than 0.2 (gray matter voxels).

Descriptive statistics for ADC and FA values was computed for the examined ROIs. Normality of the distribution was assessed using the Kolmogorov-Smirnov test.

To compare variability of data obtained by the ellipsoid ROI shape and the polygonal ROI drawing methods, the F-test was used.

Since the ADC and FA values were normally distributed (Kolmogorov-Smirnov test, $p>0.10$ for all regions), parametric statistics was employed in the analysis of intra-rater, inter-rater and between-scan reproducibility. Multiple correlation analysis with a random two-way design was used to assess intra-rater variability (five measurements of one investigator). Multivariate correlation analysis with a two-way mixed design was applied for inter-rater reproducibility (single assessments of four independent investigators). Intra-class-correlation coefficients (ICCs) were computed for ADC and FA comparisons (Shrout, 1998; Shrout and Fleiss, 1979). For comparison with literature data, the coefficient of variation (CV) was also computed according the following two equations: a) $CV_1 = \frac{\sigma}{\mu}$, ($\sigma$ standard deviation, $\mu$mean) (Bland and Altman, 1996) and b) $CV_2 = \sqrt{\frac{WSV}{\mu^2}}$ (Bland and Altman, 1996; Muller, *et al.*, 2006). Standard errors of the mean (*SEM*) of FA and ADC were computed using the formula $SEM_{WSV} = \sqrt{WSV}$, where WSV is the individual within subject (residual) variance (Bland and Altman, 1996; Muller, *et al.*, 2006).

To compare ADC and FA between the left and right hemispheres asymmetry indices (AI) for ADC and FA in all 15 examined fiber tracts, according to the formula AI = (left − right)/[(left + right)/2] were calculated (N=40 subjects). Significance of the hemispheric differences was assessed with a two-tailed paired t-test. The significance level was corrected for multiple comparisons with the Bonferroni-method.

For detection of age-related differences in ADC and FA, a univariate general linear model was used, with age and gender as independent variables.

NIH-PA Author Manuscript NIH-PA Author Manuscript NIH-PA Author Manuscript

In all tests, statistical significance was set to $P<0.05$. All analyses were performed using the SPSS software package (SPSS, Chicago, IL).

## RESULTS

Excellent data quality was achieved in all scans. Figure 3 shows the color maps from the initial examination and the repeated examination in one subject. The four slices used in the ROI analysis show good data quality and good agreement in slice position and fiber tract profile.

The F-test detected smaller variances of ADC and FA obtained by the polygonal method compared to the ellipsoidal approach. For the intra-rater data, the variance in ADC was smaller by 49% on average using the polygonal method than the ellipsoidal method (range 6.1% to −184%, significantly lower variance was detected in tracts 4 and 14, $p=0.006$ and $p<0.0001$, respectively) and the variance in FA was lower by 63% on average using the polygonal method compared to the ellipsoidal method (range −20% to −150%, significantly lower variances were found in tracts 4,6,12, and 14. $p=0.002$, $p=0.045$, $p=0.012$, and $p<0.0001$, respectively). For the inter-rater data, the average variance in ADC from the six examined regions was by 13% smaller using the polygonal method (range 40% to −98%, significantly lower variance detected in tract 14, $p=0.02$) and the average variance in FA was 51% smaller for the polygonal method (range 21% to −185%, significantly lower variances were detected in tracts 4 and 14, $p=0.02$ and $p<0.001$, respectively).

Intra-rater measurements showed excellent agreement for ADC ($ICC\geq0.99$, $p<0.001$) and FA ($ICC\geq0.97$, $p<0.001$). In the cerebral peduncle, ADC yielded $ICC\geq0.98$ ($p<0.001$), FA $ICC\geq0.96$ ($p<0.001$). The analysis yielded $CV_2$ between 0.2% and 2.7 % for ADC and FA measurements (Table 1). The repeatability (the maximal difference for 95% of pairs of measurements for the same subject (Bland and Altman, 1996)) ranged from 3 to 37 $\mu m^2/s$ for ADC (65 $\mu m^2/s$ in the cerebral peduncle, 37 $\mu m^2/s$ in the genu of the corpus callosum, and 3–6 $\mu m^2/s$ in the remaining fiber tracts). FA yielded a repeatability of 0.012–0.044. The values corresponding to an intra-rater repeatability of 95% were ≤4.3% of mean ADC values in all regions except the cerebral peduncle (repeatability 7.4%), and between 2.7% and 5.8% in for FA in all regions except the cerebral peduncle (repeatability 7.0%). Average values from both hemispheres were used.

Results on inter-rater reliability and precision are shown in Table 2. Except of the cerebral peduncle, all four investigators showed excellent agreement for ADC ($ICC\geq0.98$, $p<0.001$; genu of the corpus callosum $ICC\geq0.94$, $p<0.001$) and FA ($ICC\geq0.95$, $p<0.001$; posterior limb of the internal capsule $ICC=0.91$, $p<0.001$, genu of the corpus callosum $ICC=0.92$, $p<0.001$). In the cerebral peduncle, ADC yielded $ICC\geq0.92$ ($p<0.001$), FA $ICC\geq0.90$ ($p<0.001$). $CV_2$ estimates of inter-rater variability in ADC were in the range of 0.3%–0.4% except the cerebral peduncle ($CV_2$ 4.6%) and the genu of the corpus callosum ($CV_2$ 2.6%) and 1.9%–4.8% for FA. Inter-rater repeatability of ADC was less than 8 $\mu m^2/s$ (≤1.2% of the ADC mean) in fiber tracts other than the cerebral peduncle (114 $\mu m^2/s$, or ≤12.9% of the ADC mean) and the genu of the corpus callosum (62 $\mu m^2/s$, or ≤7.2% of the ADC mean). FA repeatability of 95% was attained at FA values less than 0.061 (≤8.4% of the FA mean) in fiber tracts other than the cerebral peduncle (0.080, or ≤13.3% of the FA mean).

Table 3 shows between-scan reliability and precision for ADC and FA. ICC values of ADC data ranged between 0.68 and 0.93 ($p<0.059$). ICC values of FA were in the range from 0.22 to 0.92 ($p<0.358$). Average $CV_2$ values of between-scan variability in ADC were in the range of 0.8%–3.4%. FA yielded CV estimates of 2.6%–5.0%. Between-scan repeatability for ADC was less than 40 $\mu m^2/s$ (≤5.6% of the ADC mean) in fiber tracts other than the cerebral peduncle (mean 72 $\mu m^2/s$, or ≤9.5% of the ADC mean) and the genu of the corpus callosum (mean 64

NIH-PA Author Manuscript NIH-PA Author Manuscript NIH-PA Author Manuscript

$\mu m^2/s$, or ≤7.8% of the ADC mean). FA repeatability was less than 0.069 (≤12.4% of the FA mean) in fiber tracts other than the cerebral peduncle (mean 0.095, or ≤14.0% of the FA mean).

Figure 5 depicts the asymmetry indices in the 15 examined fiber tracts for ADC and FA. Mean asymmetry indices lay between −4% and 9% for FA and between −6% and 3% for ADC. The average asymmetry index was 1.1%±3.3% for FA and 0.45%±2.6% for ADC. After Bonferroni correction, 6 of 15 comparisons remained significant for ADC, while four comparisons remained significant for FA (Figure 5). However, the detected hemispheric differences were of comparable or smaller magnitude than the SEMs of ADC and FA values (Table 1–3).

Figure 6 shows age-related differences of ADC and FA in the 15 examined fiber tracts. The effect of age was significant in thirteen regions: the cerebral peduncle ($R=-0.315$, $p=0.048$), temporal white matter ($R=-0.615$, $p=0.002$), frontal white matter ($R=-0.388$, $p=0.013$), anterior limb of the internal capsule ($R=-0.453$, $p=0.003$), posterior limb of the internal capsule ($R=-0.440$, $p=0.004$), splenium of the corpus callosum ($R=-0.403$, $p=0.010$), anterior white matter ($R=-0.507$, $p=0.001$), temporo-occipital white matter ($R=-0.583$, $p<0.001$), superior longitudinal fasciculus ($R=-0.661$, $p<0.001$), superior corona radiata ($R=-0.639$, $p<0.001$), superior fronto-occipital fasciculus ($R=-0.444$, $p=0.004$), cingulum ($R=-0.666$, $p<0.001$) and centrum semiovale ($R=-0.685$, $p<0.001$). The correlation coefficients between age and ADC measurements in the genu of the corpus callosum and the body of the corpus callosum were also negative, but did not reach statistical significance. In the temporal white matter, boys had 3.8% larger ADC's than girls (gender: $p=0.009$) and in the cingulum, girls had 1% larger ADCs (gender: $p=0.038$). None of the analyses showed a significant interaction term age × gender.

FA was significantly positively correlated with age in the anterior limb of the internal capsule ($R=0.488$, $p=0.001$), superior longitudinal fasciculus ($R=0.390$, $p<0.013$), and the cingulum ($R=0.324$, $p<0.042$). No fiber tract expressed significant negative correlation of FA with age. None of the analyses detected a significant effect of gender (or gender-by-age interaction).

## DISCUSSION

We investigated reproducibility, hemispheric, and age-related differences in white matter ADC and FA in healthy children and adolescents, using a clinical DTI protocol at 1.5 T. Our approach yielded an excellent intra-rater, inter-rater and between-scan reproducibility for ADC and FA. The high precision of ADC and FA measurements allowed for detection of small age-related differences in this age group. Our results indicate our experimental method and data analysis can be applied to future clinical studies.

Several factors that influence the reproducibility of DTI measures have been examined in the literature. Simulations of different noise levels and of motion introduced variations in FA (CV 15%± 1%) and ADC (CV 9%± 4%) in white matter regions (Heim, *et al.*, 2004). Examinations performed on the same scanner had inherent variation that affected FA (CV 1.9%) and ADC (CV 2.6 %) less than examinations performed on different scanner systems (CV: FA, 4.5%; ADC, 7.5%) (Pfefferbaum, *et al.*, 2003). Diffusion tractography was used to determine FA reproducibility in the anterior callosal fibers, optic radiations, and pyramidal tracts for the same operator (n=6, CV 1.2%– 2.9%), between operators (n=6, CV 2.6%– 3.8%) and in comparison to a second scan after 3 to 6 months (n=4, CV 5.0%– 7.1%) (Ciccarelli, *et al.*, 2003). Intraobserver reliability (ICC ≥ 0.90) and precision (CV ≤ 3.5%) of hippocampal rectangular ROI measurements of FA and ADC (n=20) was higher than interobserver reliability (ICC ≥ 0.84; CV ≤ 4.1%). CI95 was determined ±0.015–0.020 for FA and ±25–30 $\mu m^2/s$ for ADC, such that a detectable difference of 0.020–0.030 for FA and 40–50 $\mu m^2/s$ for ADC could be assumed (Muller, *et al.*, 2006).

NIH-PA Author Manuscript NIH-PA Author Manuscript NIH-PA Author Manuscript

In our study, both intra-rater and inter-rater comparisons revealed nearly twofold higher variability for FA values (mean $CV_2$ 1.90% and 3.22%, respectively) compared to ADC measurements (mean $CV_2$ 1.06%, and 1.66%, respectively). The CV values found in this study are in agreement with data reported by other studies with different designs and methodology (Heim, *et al.*, 2004; Muller, *et al.*, 2006; Pfefferbaum, *et al.*, 2003; Snook, *et al.*, 2005). In accordance with previous studies, inter-rater precision was approximately one third lower than the precision of repeated measurements derived from one single observer (Ciccarelli, *et al.*, 2003; Muller, *et al.*, 2006). A higher reproducibility of ADC measurements in this study is also consistent with previous findings (Heim, *et al.*, 2004). In the healthy brain, white matter and gray matter have very similar ADC values, and as a result the ADC distribution is very homogenous throughout the brain, whereas FA exhibits distinct mean values between white and gray matter (Basser and Pajevic, 2000). This may explain inaccuracies of FA measures due to partial volume effects and ROI outlines of fiber tracts close to their borders. A similar problem exists for ADC in regions close to cerebrospinal fluid or with a small diameter, which is demonstrated by the increased variability of measurements in the cerebral peduncle and the genu of the corpus callosum. It can be assumed that a more restricted ROI outline than shown in Figure 2a may help to increase the reliability of DTI parameter estimates in the cerebral peduncle. However, part of the variability of the DTI parameter estimates in the cerebral peduncle may also be due to the lower image quality in this region, mostly caused by the susceptibility differences of the surrounding bones and air spaces of the nasopharynx.

The between-scan analysis showed lower ICCs compared to the intra-rater and inter-rater ICCs than expected by the excellent coefficients of variation and repeatability estimates in the between-scan analysis. For example, data from the right anterior limb of the internal capsule show that in the between-scan analysis, the ADC estimates that correspond to 95% repeatability in the right anterior limb of the internal capsule were 35 $\mu m^2/s$, compared to 10 $\mu m^2/s$ in the inter-rater analysis and 9 $\mu m^2/s$ in the intra-rater analysis.

Rater performance is an important source of variability in the data and is one of the limiting factors in detection of normal and pathological variance in both cross-sectional and longitudinal studies. The sources of variability are specific for the (individual or group of) raters, whose performance depends on the adequacy of the set rules for anatomic delineations and the skills of the raters to follow these rules. We tried to minimize the impact of these effects by adequately training and supervising the raters. Two of the raters (including the rater evaluating data for intra-rater reproducibility and between-scan reproducibility) had previous experience with processing DTI data for other projects. Additional sources of error contribute to data variability: signal-to-noise level, gradient stability, motion during the scans, and differences in slice position between subjects (contributing to noise in data in cross-sectional and longitudinal studies) and between examinations (contributing to noise in data in longitudinal studies). During the examinations, we carefully positioned the subjects and instructed them to hold still during the scan to minimize motion artifacts. All the discussed factors (rater- and experiment-related) affect both cross-sectional and longitudinal data; however, the longitudinal studies are preferable due to a larger power to detect between-group differences with the same number of subjects.

In our analyses, we used FA=0.2 to define the boundary of the ROIs. However, if FA were largely decreased in areas of pathology, the method might provide ROIs that are too small. Therefore, for FA evaluations in pathology, it is necessary to carefully inspect both FA values and the size of the ROIs. An alternative approach to guard against partial volume effects may be the use of ROI erosion/dilation methods.

Significant hemispheric asymmetries were found in 6 of 15 fiber tracts for ADC and 4 of 15 fiber tracts for FA (Figure 5). In children, Klingberg et al. (Klingberg, *et al.*, 1999) found a

NIH-PA Author Manuscript NIH-PA Author Manuscript NIH-PA Author Manuscript

larger FA in the right hemisphere in central white matter of the frontal lobe while we detected rightward asymmetry in a more anterior region (region 3) and no asymmetry in the corresponding central region in the frontal lobe (region 9). Our findings of leftward asymmetry of FA in centrum semiovale correspond to previously reported results (Snook, *et al.*, 2005); however, we did not detect any asymmetry in the anterior limb of the internal capsule in our subjects. In agreement with previous observations, the hemispheric differences were small in magnitude (Snook, *et al.*, 2005) and comparable to the operator variability (Tables 1–3). The absolute values of the differences were mainly below 10 $\mu m/s^2$ for ADC and below 0.010 for FA. Possibly, small hemispheric differences found by assessments in one slice may be attributable to slight slice angulation, such that the fiber tract is not measured at the same level and with the same partial volume averaging on both sides. Since determination of DTI parameters depends on slice position and orientation, keeping the same slice position and orientation in longitudinal measurements is essential (Virta, *et al.*, 1999).

Age effects can be observed during the development of the brain and during adaptations and decline in cognitive function later in life. The largest age related variation in DTI parameters has been shown in newborns and infants younger than 3 years (Jones, *et al.*, 2003; Hermoye, *et al.*, 2006). The changes of ADC and FA after the first 24 months of life are small (Hermoye, *et al.*, 2006), so that a sensitive methodology is necessary to detect the age effect. In agreement with literature data, we found significant age-related differences in ADC and FA in our group of children and adolescents. In children 8 to 13 years old ADC has been determined between 7.0 and 8.0 × 10–4 $mm^2/s$ (Snook, et al., 2005) in the anterior limb of the internal capsule with a significant decrease with age. In another study, ADC values of 8–9 × $10^{-4}$ $mm^2/s$ were determined for the period between 12 and 60 months of life (Hermoye, et al., 2006). In agreement with a voxel-based study (Schmithorst, *et al.*, 2002) widespread areas of the white matter showed negative correlation of the ADC measurements with age. FA findings are potentially more difficult to compare due to potential variability and errors associated with ROI placement. When ROIs are outlined on the color maps instead of on T2-weighted scans, the ROI is more likely to contain a pure sample of white matter and a higher FA average. However, our FA data show a good agreement with literature values in corresponding brain regions for young children (Hermoye, *et al.*, 2006). In agreement with a voxel-based approach (Barnea-Goraly, *et al.*, 2005) we found a significant positive correlation of FA with age in the anterior limb of the internal capsule, the superior longitudinal fasciculus, and the cingulum. Another voxel based study in children and adolescents reported positive correlation between FA and age (Schmithorst, *et al.*, 2002). In contrast to our study, no significant findings in the superior longitudinal fasciculus or cingulum were detected. The external capsule, inferior longitudinal fasciculus and arcuate fasciculus showing significant positive correlation with age (Schmithorst, *et al.*, 2002) were not included in our study. In contrast to previous findings (Schmithorst, *et al.*, 2002), we did not detect any significant negative correlation between FA and age. The reported significant negative correlation of FA (and positive correlation of ADC) with age (Schmithorst, *et al.*, 2002) may be due to a large number of comparisons involved in voxel-based analysis, which may lead to an increase of the false positive findings. Comparison of our FA data to white matter FA in elderly subjects (FA decrease from 0.30 to 0.24 in the age range between 50 and 90 years) (Charlton, *et al.*, 2006) revealed a higher average value in our study (pooled data of all examined fiber tracts: FA = 0.58±0.12). The difference may be due to continuous age-related white matter changes between young adulthood and advanced age.

Although we detected significant age-related differences in ADC in 13 regions, only 3 regions showed a significant correlation between FA and age. This result may be explained in part by a better reproducibility of ADC measurements compared to FA measurements in our study. It should also be considered that if the eigenvalues $\lambda_{\parallel}$ and $\lambda_{\perp}$ of the diffusion tensor would change in the same direction no age-related differences in FA may be observed. In such cases,

NIH-PA Author Manuscript NIH-PA Author Manuscript NIH-PA Author Manuscript

evaluation of $\lambda_{\parallel}$ and $\lambda_{\perp}$ in addition to FA may be of advantage (Budde, *et al.*, 2006). In our study, the age-related decrease in FA in tract 11 can be explained by a decrease in all eigenvalues (linear regression analysis, all $p<0.006$) and in tracts 4 and 14 by a decrease in the two $\lambda_{\perp}$ values ($p<0.001$). For the FA in regions that did not show a significant effect of age, all eigenvalues decreased with age in regions 10, 12, 13, and 15 ($p<0.035$). In regions 2, 5, and 9, a decrease in $\lambda_{\parallel}$ was accompanied by a decrease in one $\lambda_{\perp}$ ($p<0.03$) and in regions 3, 6, 7, and 8, only a significant decrease in $\lambda_{\parallel}$ was detected ($p<0.03$). No significant decrease in any of the eigenvalues was observed in region 1 ($\lambda_{\perp}$ tended to decrease with age, $p=0.056$).

The developmental increase of FA and decrease of ADC during childhood corresponds to increased myelination and thickening of the axon diameter (Sakuma, *et al.*, 1991). Agreement in findings between DTI studies in infancy and early childhood (Hermoye, *et al.*, 2006) and histological examination (Brody, *et al.*, 1987; Kinney, *et al.*, 1988) support myelination as an important factor affecting FA and ADC. Myelination was found to contribute to a 25–30% increase in anisotropy (Zhang, *et al.*, 2003; Zhang, *et al.*, 2005). However, high anisotropy has also been found in non- and pre-myelinated embryonic and neonate brains (Pierpaoli and Basser, 1996; Dubois, *et al.*, 2006). It has also been proposed that water loss induced by the development of the hydrophobic inner layer of the myelin sheath contributes to decreases in ADC and changes in the anisotropy of diffusion (Barkovich, *et al.*, 1988). Reduction in water content and increase of cohesiveness and compactness of the fiber tracts (McGraw, *et al.*, 2002) and a reduction in extra-axonal space (Beaulieu and Allen, 1994) are additional components of brain maturation affecting DTI parameters. ADC and FA can also be affected by changes in the organization of nerve fibers (Alexander, *et al.*, 2001). Also, the differences of average brain size in different age groups in pediatric populations are commonly assessed with MRI protocols with a fixed voxel size, therefore introducing variation in the amount of partial volume averaging in the data (Alexander, *et al.*, 2001).

The fiber tracts examined in our study represent common targets of pathology. They have well known anatomy, are easily identifiable and comprise a selection of diverse fiber characteristics and orientations. When interpreting the results of this study it has to be considered that the only operator dependent step in the intra-rater and inter-rater analyses was the subjective placement of the ROIs. All other computations were carried out fully automated. In the between-scan analysis, we intended to minimize the subjective effect by having the operator place the ROIs on pairs of fiber tracts simultaneously. Our results show a high precision of ADC and FA measurements that enabled us to detect small age-related differences, despite of DTI acquisition parameter constraints and data acquisition at the end of a relatively long pediatric clinical MR protocol.

**Acknowledgements**

This study was supported by NIH grant 1RO1 NS042851-01A2 and the Johns Hopkins General Clinical Research Center (NIH M01 RR 00052). We thank Dr. Hangyi Jiang, Dr. Craig Jones and Dr. Jonathan Farrell for software support. We also would like to thank Rena Geckle and Amanda Barnes for their help with recruitment of subjects and Cynthia Schultz for help with data acquisition.

## References

Alexander AL, Hasan KM, Lazar M, Tsuruda JS, Parker DL. Analysis of partial volume effects in diffusion-tensor MRI. Magn Reson Med 2001;45:770–80. [PubMed: 11323803]

Barkovich AJ, Kjos BO, Jackson DE Jr, Norman D. Normal maturation of the neonatal and infant brain: MR imaging at 1.5 T. Radiology 1988;166:173–80. [PubMed: 3336675]

Barnea-Goraly N, Menon V, Eckert M, Tamm L, Bammer R, Karchemskiy A, Dant CC, Reiss AL. White matter development during childhood and adolescence: a cross-sectional diffusion tensor imaging study. Cereb Cortex 2005;15:1848–54. [PubMed: 15758200]

NIH-PA Author Manuscript NIH-PA Author Manuscript NIH-PA Author Manuscript

Basser PJ, Mattiello J, LeBihan D. Estimation of the effective self-diffusion tensor from the NMR spin echo. J Magn Reson B 1994;103:247–54. [PubMed: 8019776]

Basser PJ, Mattiello J, LeBihan D. MR diffusion tensor spectroscopy and imaging. Biophys J 1994;66:259–67. [PubMed: 8130344]

Basser PJ, Pajevic S. Statistical artifacts in diffusion tensor MRI (DT-MRI) caused by background noise. Magn Reson Med 2000;44:41–50. [PubMed: 10893520]

Basser PJ, Pierpaoli C. A simplified method to measure the diffusion tensor from seven MR images. Magn Reson Med 1998;39:928–34. [PubMed: 9621916]

Beaulieu C, Allen PS. Determinants of anisotropic water diffusion in nerves. Magn Reson Med 1994;31:394–400. [PubMed: 8208115]

Bland JM. Altman DG. Measurement error. BMJ 1996;313:744. [PubMed: 8819450]

Bland JM, Altman DG. Measurement error proportional to the mean. BMJ 1996;313:106. [PubMed: 8688716]

Bonekamp D, Nagae-Poetscher LM, Degaonkar M, Matson M, Mori S, Horska A. Intra-rater and inter-rater reproducibility of FA and ADC: a clinical pediatric DTI study. Proc Int Soc Magn Res Med 2005;147

Briellmann RS, Mitchell LA, Waites AB, Abbott DF, Pell GS, Saling MM, Jackson GD. Correlation between language organization and diffusion tensor abnormalities in refractory partial epilepsy. Epilepsia 2003;44:1541–5. [PubMed: 14636325]

Brody BA, Kinney HC, Kloman AS, Gilles FH. Sequence of central nervous system myelination in human infancy. I. An autopsy study of myelination. J Neuropathol Exp Neurol 1987;46:283–301. [PubMed: 3559630]

Budde MD, Kim JH, Liang H-F, Schmidt RE, Russell JH, Cross AH, Song S-K. Toward Accurate Diagnosis of White Matter Pathology Using Diffusion Tensor Imaging. Proc Int Soc Magn Res Med 2006;24

Cassol E, Ranjeva JP, Ibarrola D, Mekies C, Manelfe C, Clanet M, Berry I. Diffusion tensor imaging in multiple sclerosis: a tool for monitoring changes in normal-appearing white matter. Mult Scler 2004;10:188–96. [PubMed: 15124766]

Charlton RA, Barrick TR, McIntyre DJ, Shen Y, O'Sullivan M, Howe FA, Clark CA, Morris RG, Markus HS. White matter damage on diffusion tensor imaging correlates with age-related cognitive decline. Neurology 2006;66:217–22. [PubMed: 16434657]

Ciccarelli O, Parker GJ, Toosy AT, Wheeler-Kingshott CA, Barker GJ, Boulby PA, Miller DH, Thompson AJ. From diffusion tractography to quantitative white matter tract measures: a reproducibility study. Neuroimage 2003;18:348–59. [PubMed: 12595188]

Dubois J, Hertz-Pannier L, Dehaene-Lambertz G, Cointepas Y, Le Bihan D. Assessment of the early organization and maturation of infants' cerebral white matter fiber bundles: A feasibility study using quantitative diffusion tensor imaging and tractography. Neuroimage 2006;30:1121–32. [PubMed: 16413790]

Heim S, Hahn K, Samann PG, Fahrmeir L, Auer DP. Assessing DTI data quality using bootstrap analysis. Magn Reson Med 2004;52:582–9. [PubMed: 15334578]

Hermoye L, Saint-Martin C, Cosnard G, Lee SK, Kim J, Nassogne MC, Menten R, Clapuyt P, Donohue PK, Hua K, Wakana S, Jiang H, van Zijl PC, Mori S. Pediatric diffusion tensor imaging: normal database and observation of the white matter maturation in early childhood. Neuroimage 2006;29:493–504. [PubMed: 16194615]

Jones DK, Horsfield MA, Simmons A. Optimal strategies for measuring diffusion in anisotropic systems by magnetic resonance imaging. Magn Reson Med 1999;42:515–25. [PubMed: 10467296]

Jones RA, Palasis S, Grattan-Smith JD. The evolution of the apparent diffusion coefficient in the pediatric brain at low and high diffusion weightings. J Magn Reson Imaging 2003;18:665–74. [PubMed: 14635151]

Kinney HC, Brody BA, Kloman AS, Gilles FH. Sequence of central nervous system myelination in human infancy. II. Patterns of myelination in autopsied infants. J Neuropathol Exp Neurol 1988;47:217–34. [PubMed: 3367155]

NIH-PA Author Manuscript NIH-PA Author Manuscript NIH-PA Author Manuscript

Klingberg T, Vaidya CJ, Gabrieli JD, Moseley ME, Hedehus M. Myelination and organization of the frontal white matter in children: a diffusion tensor MRI study. Neuroreport 1999;10:2817–21. [PubMed: 10511446]

McGraw P, Liang L, Provenzale JM. Evaluation of normal age-related changes in anisotropy during infancy and childhood as shown by diffusion tensor imaging. AJR Am J Roentgenol 2002;179:1515–22. [PubMed: 12438047]

Miller JH, McKinstry RC, Philip JV, Mukherjee P, Neil JJ. Diffusion-tensor MR imaging of normal brain maturation: a guide to structural development and myelination. AJR Am J Roentgenol 2003;180:851–9. [PubMed: 12591710]

Mukherjee P, Miller JH, Shimony JS, Conturo TE, Lee BC, Almli CR, McKinstry RC. Normal brain maturation during childhood: developmental trends characterized with diffusion-tensor MR imaging. Radiology 2001;221:349–58. [PubMed: 11687675]

Muller MJ, Mazanek M, Weibrich C, Dellani PR, Stoeter P, Fellgiebel A. Distribution characteristics, reproducibility, and precision of region of interest-based hippocampal diffusion tensor imaging measures. AJNR Am J Neuroradiol 2006;27:440–6. [PubMed: 16484426]

Pajevic S, Pierpaoli C. Color schemes to represent the orientation of anisotropic tissues from diffusion tensor data: application to white matter fiber tract mapping in the human brain. Magn Reson Med 1999;42:526–40. [PubMed: 10467297]

Pfefferbaum A, Adalsteinsson E, Sullivan EV. Replicability of diffusion tensor imaging measurements of fractional anisotropy and trace in brain. J Magn Reson Imaging 2003;18:427–33. [PubMed: 14508779]

Pierpaoli C, Basser PJ. Toward a quantitative assessment of diffusion anisotropy. Magn Reson Med 1996;36:893–906. [PubMed: 8946355]

Reich, W.; Welner, Z.; Herjanic, B. The Diagnostic Interview for Children and Adolescents-IV. North Tonawanda: Multi-Health Systems; 1997.

Sakuma H, Nomura Y, Takeda K, Tagami T, Nakagawa T, Tamagawa Y, Ishii Y, Tsukamoto T. Adult and neonatal human brain: diffusional anisotropy and myelination with diffusion-weighted MR imaging. Radiology 1991;180:229–33. [PubMed: 2052700]

Schmithorst VJ, Wilke M, Dardzinski BJ, Holland SK. Correlation of white matter diffusivity and anisotropy with age during childhood and adolescence: a cross-sectional diffusion-tensor MR imaging study. Radiology 2002;222:212–8. [PubMed: 11756728]

Shrout PE. Measurement reliability and agreement in psychiatry. Statistical Methods in Medical Research 1998;7:301–17. [PubMed: 9803527]

Shrout PE, Fleiss JL. Intraclass correlations: Uses in assessing rater reliability. Psychol Bulletin 1979;86:420–28.

Snook L, Paulson LA, Roy D, Phillips L, Beaulieu C. Diffusion tensor imaging of neurodevelopment in children and young adults. Neuroimage 2005;26:1164–73. [PubMed: 15961051]

Sun Z, Wang F, Cui L, Breeze J, Du X, Wang X, Cong Z, Zhang H, Li B, Hong N, Zhang D. Abnormal anterior cingulum in patients with schizophrenia: a diffusion tensor imaging study. Neuroreport 2003;14:1833–6. [PubMed: 14534430]

Virta A, Barnett A, Pierpaoli C. Visualizing and characterizing white matter fiber structure and architecture in the human pyramidal tract using diffusion tensor MRI. Magn Reson Imaging 1999;17:1121–33. [PubMed: 10499674]

Wakana S, Jiang H, Nagae-Poetscher LM, van Zijl PC, Mori S. Fiber tract-based atlas of human white matter anatomy. Radiology 2004;230:77–87. [PubMed: 14645885]

Welner Z, Reich W, Herjanic B, Jung KG, Amado H. Reliability, validity, and parent-child agreement studies of the Diagnostic Interview for Children and Adolescents (DICA). J Am Acad Child Adolesc Psychiatry 1987;26:649–53. [PubMed: 3667494]

Zhang J, Miller MI, Plachez C, Richards LJ, Yarowsky P, van Zijl P, Mori S. Mapping postnatal mouse brain development with diffusion tensor microimaging. Neuroimage 2005;26:1042–51. [PubMed: 15961044]

Zhang J, Richards LJ, Yarowsky P, Huang H, van Zijl PC, Mori S. Three-dimensional anatomical characterization of the developing mouse brain by diffusion tensor microimaging. Neuroimage 2003;20:1639–48. [PubMed: 14642474]

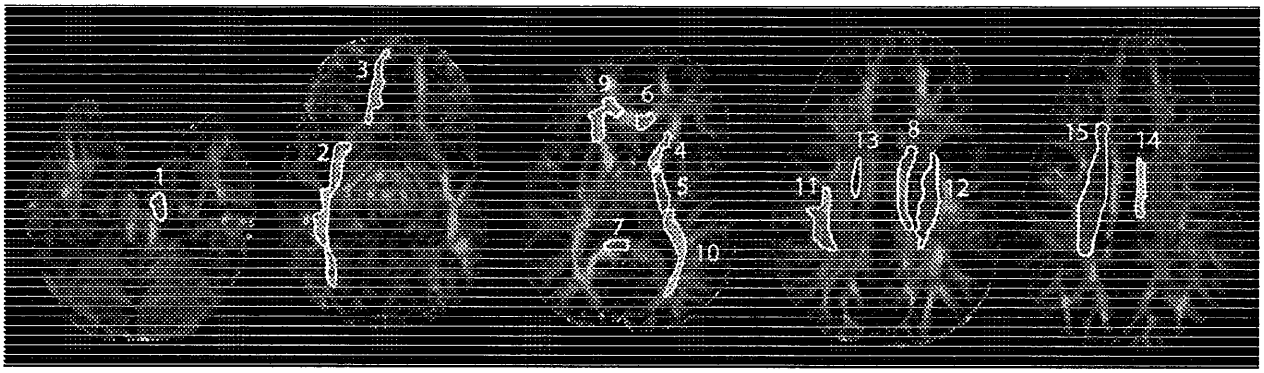


**Figure 1. ROIs for study of age-related changes**

Fifteen regions of interest used to study age-related changes in DTI parameters overlaid on color map slices. CP (1): cerebral peduncle, TWM (2): temporal white matter. FWM (3): frontal white matter. ALIC (4): anterior limb of the internal capsule, PLIC (5): posterior limb of the internal capsule. GCC (6): genu, SCC (7): splenium, BCC (8): body of the corpus callosum. AWM (9): anterior white matter, TOWM (10): temporo-occipital white matter, SLF (11): superior longitudinal fasciculus. SCR (12): superior corona radiata, SFOF (13): superior fronto-occipital fasciculus. CING (14): cingulum. CSO (15): centrum semiovale.



NEURO00036268

NIH-PA Author Manuscript NIH-PA Author Manuscript NIH-PA Author Manuscript

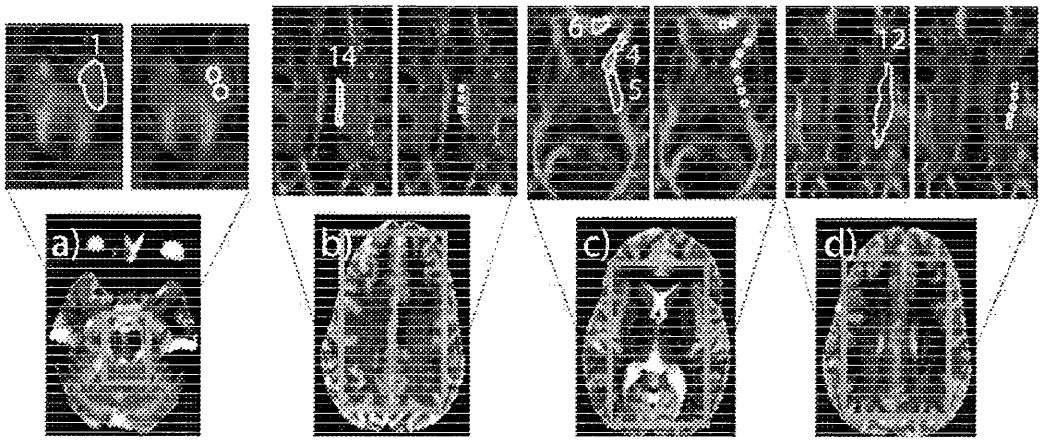


**Figure 2. ROIs for reproducibility analysis**

Upper panel: Regions of interest (ROIs) are shown overlaid on the color map: polygonal ROIs are displayed on the left side, ellipsoid ROIs on the right side. Lower panel: The location of the color map is shown on the corresponding T2 weighted image. The following ROIs were evaluated: a) from top to bottom: genu of the corpus callosum (6), anterior limb of the internal capsule (4), posterior limb of the internal capsule (5), b) superior corona radiata (12), c) cerebral peduncle (1), d) cingulum (14). Numbers in brackets relate these ROIs to the 15 ROIs in Figure 1.



NIH-PA Author Manuscript NIH-PA Author Manuscript NIH-PA Author Manuscript

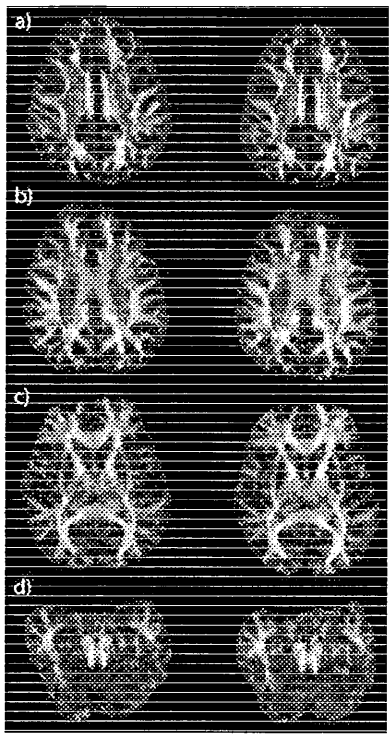


**Figure 3. Scan – rescan - comparison**

Color-coded FA maps of initial scan (left panel) and repeated scan (right panel, 3 days later) from a 17.9 year old male. Of the 22 acquired slices, the four slices used in the ROI analysis are shown; slices depict a) cingulum b) superior corona radiata c) anterior and posterior limb of the internal capsule, genu of the corpus callosum, d) cerebral peduncle.



NIH-PA Author Manuscript NIH-PA Author Manuscript NIH-PA Author Manuscript

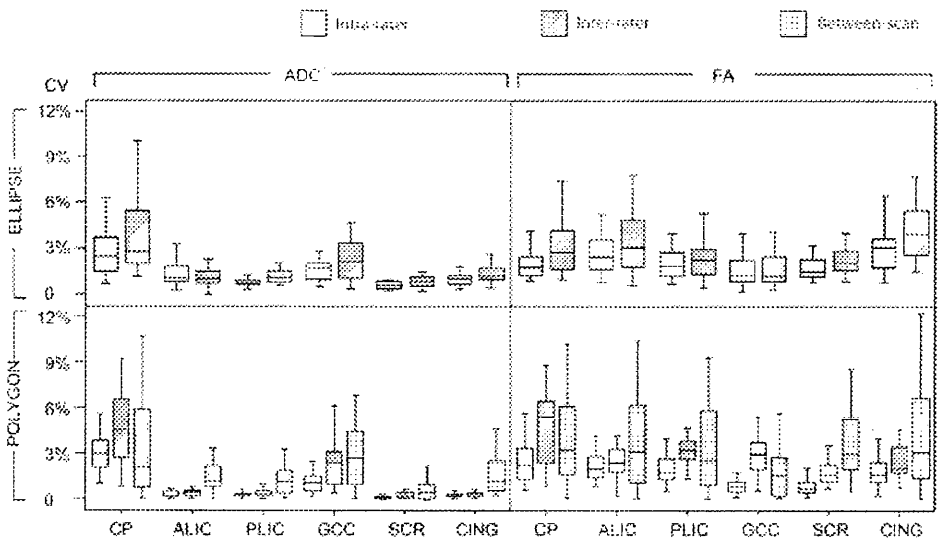


**Figure 4. Intra-, inter-rater and between-scan reproducibility of measurements of ADC and FA**

Coefficients of variation ($CV_1$, see text) are depicted as boxplots, N=20, pooled data for right and left measurements. Data are shown for each tract (abscissa); ROIs are identified in the caption of Figure 1. Separate diagrams are shown for the ellipsoid ROI method (upper half) and the polygonal method (lower half). ADC measurements are shown in the left half of the diagram, FA measurements in the right half of the diagram. Intra-rater and inter-rater reproducibility are shown for the ellipsoid ROI approach, intra-rater, inter-rater and between-scan $CV_1$s are shown for the polygonal ROI approach. The polygonal ROI method has significant better reproducibility (lower $CV_1$ values) than the ellipsoid approach, both for ADC and FA and for intra- and inter-rater measurements. The intra-rater measurements have lower $CV_1$ values than those between different operators. The between-scan reproducibility analysis yields significantly higher $CV_1$ for ADC values when compared to intra- ($p<.001$) and inter-rater ($p=.043$) results. FA reproducibility was significantly better in the intra-rater analysis ($p<.001$), but not in the inter-rater analysis ($p=.084$), when compared to the between-scan analysis. ADC generally shows better reproducibility than FA.



NIH-PA Author Manuscript NIH-PA Author Manuscript NIH-PA Author Manuscript

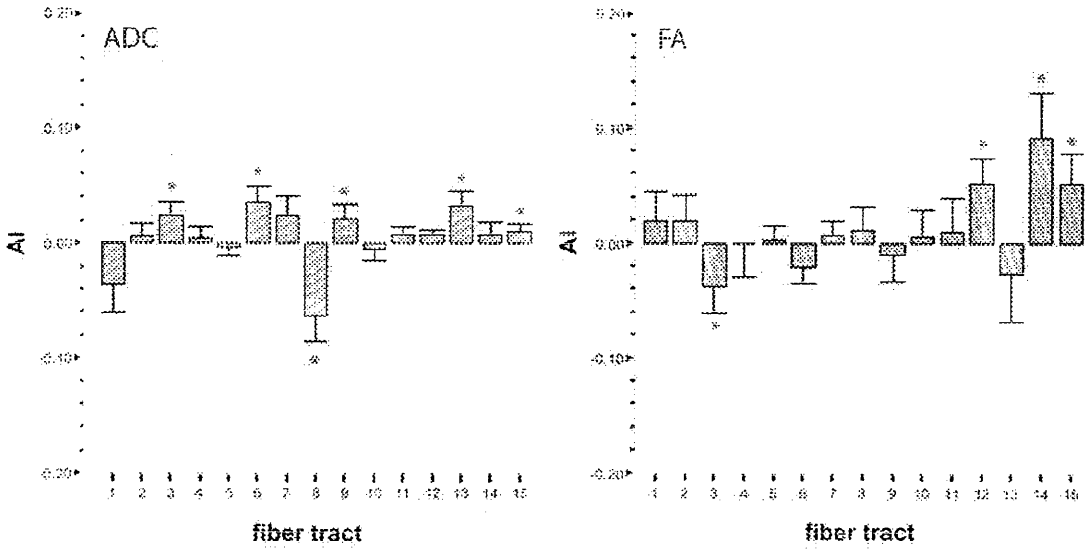


**Figure 5. Asymmetry indices**

Mean values and standard deviations of asymmetry indices calculated for each region. Regions are represented by numbers as given in the caption of Figure 1. Asterisk (*) indicates P<0.05 after Bonferroni-correction.

NIH-PA Author Manuscript

NIH-PA Author Manuscript

NIH-PA Author Manuscript

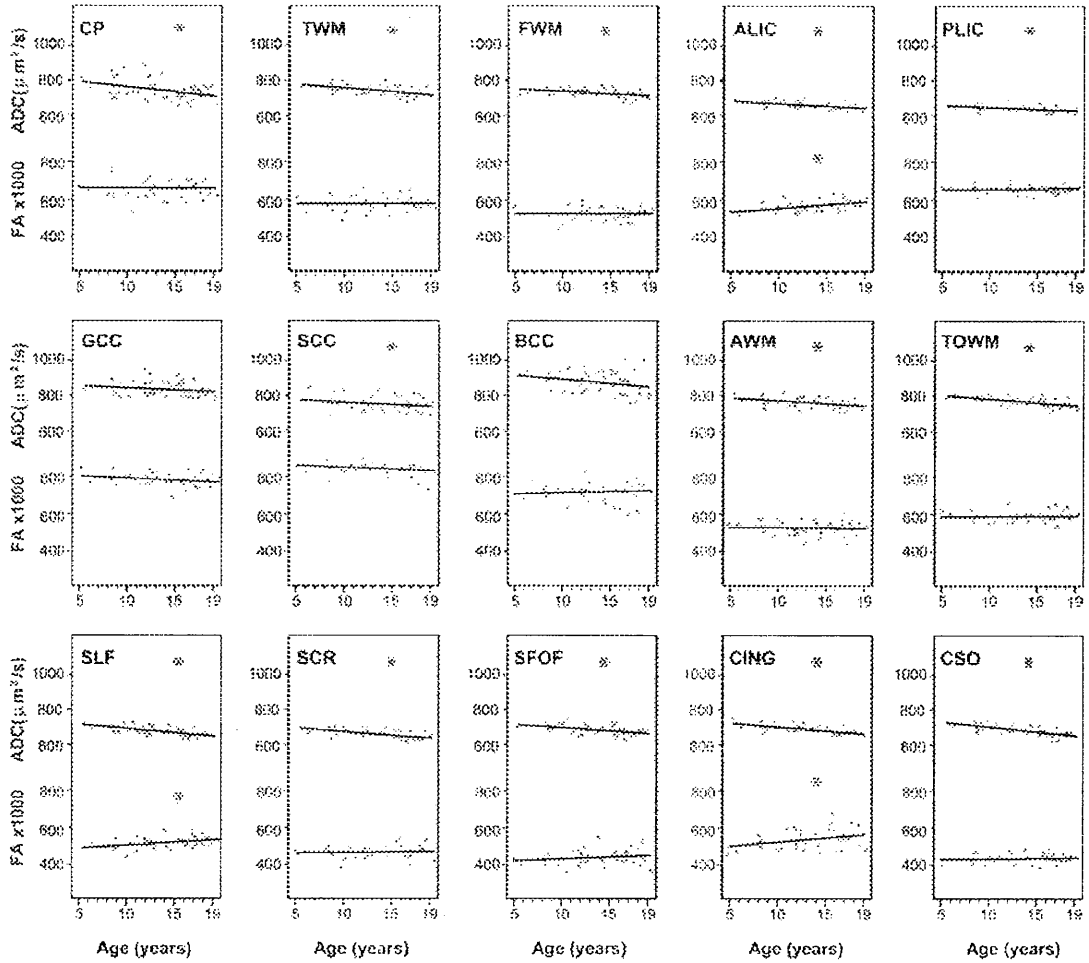


**Figure 6. Age-related differences**

Scatter plots for all 15 examined fiber tracts of age (abscissa) and DTI parameter (ordinate). FA (scaled by a factor of 1000); ADC ($\mu m^2/s$). ROIs are identified as given in the caption of Figure 1. Asterisk (*) indicates significant correlations.



NIH-PA Author Manuscript NIH-PA Author Manuscript NIH-PA Author Manuscript

NIH-PA Author Manuscript NIH-PA Author Manuscript NIH-PA Author Manuscript



**Table 1**

Intra-rater reproducibility and precision of measurements in 6 examined fiber tracts (N=10).

| | | Measurement (Mean ± SD) | | | | | | | | |
|---|---|---|---|---|---|---|---|---|---|---|
| | | 1st | 2nd | 3rd | 4th | 5th | ICC | SEM | CI 95% | CV2 | R95 (%) |
| CP | ADC mean | 881 ± 64 | 874 ± 78 | 875 ± 85 | 866 ± 70 | 862 ± 73 | 0.98 | 23.4 | ±46 | 2.7% | 65 (7.4%) |
| ALIC | ADC mean | 703 ± 17 | 703 ± 17 | 703 ± 17 | 705 ± 17 | 705 ± 18 | 1.00 | 2.3 | ±5 | 0.3% | 6 (0.9%) |
| PLIC | ADC mean | 679 ± 10 | 678 ± 10 | 679 ± 10 | 679 ± 11 | 679 ± 10 | 0.99 | 2.0 | ±4 | 0.3% | 6 (0.8%) |
| GCC | ADC mean | 864 ± 53 | 858 ± 60 | 856 ± 58 | 850 ± 53 | 848 ± 44 | 0.99 | 13.3 | ±26 | 1.5% | 37 (4.3%) |
| SCR | ADC mean | 690 ± 17 | 689 ± 16 | 690 ± 17 | 689 ± 17 | 689 ± 17 | 1.00 | 1.1 | ±2 | 0.2% | 3 (0.5%) |
| CING | ADC mean | 708 ± 10 | 708 ± 11 | 709 ± 11 | 710 ± 11 | 709 ± 11 | 0.99 | 1.9 | ±4 | 0.3% | 5 (0.7%) |
| CP | FA mean | 626 ± 39 | 635 ± 44 | 641 ± 37 | 643 ± 38 | 646 ± 39 | 0.96 | 16.0 | ±31 | 2.5% | 44 (7.0%) |
| ALIC | FA mean | 514 ± 32 | 529 ± 31 | 525 ± 30 | 526 ± 29 | 529 ± 33 | 0.97 | 10.9 | ±21 | 2.1% | 30 (5.8%) |
| PLIC | FA mean | 592 ± 32 | 608 ± 31 | 602 ± 33 | 603 ± 32 | 607 ± 33 | 0.97 | 11.9 | ±23 | 2.0% | 33 (5.5%) |
| GCC | FA mean | 751 ± 44 | 755 ± 43 | 755 ± 39 | 752 ± 36 | 756 ± 36 | 0.99 | 7.5 | ±15 | 1.0% | 21 (2.8%) |
| SCR | FA mean | 435 ± 25 | 438 ± 25 | 438 ± 26 | 440 ± 27 | 439 ± 25 | 0.99 | 4.3 | ±8 | 1.0% | 12 (2.7%) |
| CING | FA mean | 465 ± 34 | 474 ± 29 | 474 ± 28 | 475 ± 35 | 476 ± 32 | 0.99 | 7.8 | ±15 | 1.6% | 22 (4.6%) |

Abbreviations: FA, fractional anisotropy ($\times 10^3$); ADC, apparent diffusion coefficient ($\mu m^2$ s); ICC, intraclass correlation coefficient; SEM, standard error of measurement based on within-subject variance; CI 95%, 95% confidence interval; CV2, coefficient of variation; R95, repeatability. Fiber tracts: CP, cerebral peduncle; ALIC, anterior limb of internal capsule; PLIC, posterior limb of internal capsule; GCC, genu of corpus callosum; SCR, superior corona radiata; CING: cingulum. Data include polygonal ROI method only.



NEURO00036274

NIH-PA Author Manuscript NIH-PA Author Manuscript NIH-PA Author Manuscript



**Table 2**

Inter-rater reproducibility and precision of measurements in 6 examined fiber tracts (N=10).

| | | Mean ± SD | | | | ICC | SEM | CI 95% | CV2 | R95 (%) |
|---|---|---|---|---|---|---|---|---|---|---|
| | | Operator 1 | Operator 2 | Operator 3 | Operator 4 | | | | | |
| CP | ADC mean | 881 ± 64 | 888 ± 63 | 884 ± 92 | 889 ± 103 | 0.92 | 41.1 | ±81 | 4.6% | 114 (12.9%) |
| ALIC | ADC mean | 703 ± 17 | 702 ± 16 | 704 ± 16 | 702 ± 17 | 0.99 | 3.0 | ±6 | 0.4% | 8 (1.2%) |
| PLIC | ADC mean | 679 ± 10 | 678 ± 11 | 677 ± 10 | 678 ± 12 | 0.98 | 2.7 | ±5 | 0.4% | 7 (1.1%) |
| GCC | ADC mean | 864 ± 53 | 881 ± 47 | 853 ± 49 | 863 ± 42 | 0.94 | 22.5 | ±44 | 2.6% | 62 (7.2%) |
| SCR | ADC mean | 690 ± 17 | 689 ± 17 | 687 ± 15 | 688 ± 16 | 0.99 | 2.9 | ±6 | 0.4% | 8 (1.2%) |
| CTNG | ADC mean | 708 ± 10 | 708 ± 11 | 707 ± 10 | 706 ± 9 | 0.99 | 2.3 | ±5 | 0.3% | 6 (0.9%) |
| CP | FA mean | 626 ± 39 | 573 ± 50 | 609 ± 50 | 602 ± 49 | 0.90 | 29.0 | ±57 | 4.8% | 80 (13.3%) |
| ALIC | FA mean | 514 ± 32 | 519 ± 31 | 517 ± 28 | 530 ± 29 | 0.95 | 12.3 | ±24 | 2.4% | 34 (6.6%) |
| PLIC | FA mean | 592 ± 32 | 594 ± 29 | 621 ± 29 | 599 ± 34 | 0.91 | 17.8 | ±35 | 3.0% | 49 (8.2%) |
| GCC | FA mean | 751 ± 44 | 714 ± 39 | 723 ± 41 | 746 ± 38 | 0.92 | 22.1 | ±43 | 3.0% | 61 (8.4%) |
| SCR | FA mean | 435 ± 25 | 429 ± 26 | 443 ± 26 | 431 ± 27 | 0.97 | 8.4 | ±17 | 1.9% | 23 (5.4%) |
| CTNG | FA mean | 465 ± 34 | 464 ± 36 | 480 ± 44 | 479 ± 34 | 0.96 | 14.0 | ±28 | 3.0% | 39 (8.2%) |

Abbreviations are listed in Table 1.

**Table 3**

Between-scan reproducibility and precision of measurements in 6 examined fiber tracts (N=10).

| | | Initial | Rescan | ICC | SEM | CI 95% | CV2 | R95 (%) |
|---|---|---|---|---|---|---|---|---|
| CP | ADC mean | 750 ± 51 | 760 ± 54 | 0.86 | 26.0 | ±51 | 3.4% | 72 (9.5%) |
| ALIC | ADC mean | 684 ± 14 | 685 ± 19 | 0.73 | 10.5 | ±21 | 1.5% | 29 (4.3%) |
| PLIC | ADC mean | 662 ± 13 | 660 ± 18 | 0.82 | 8.5 | ±17 | 1.3% | 24 (3.6%) |
| GCC | ADC mean | 817 ± 36 | 824 ± 32 | 0.68 | 23.1 | ±45 | 2.8% | 64 (7.8%) |
| SCR | ADC mean | 665 ± 15 | 663 ± 13 | 0.93 | 5.2 | ±10 | 0.8% | 14 (2.2%) |
| CING | ADC mean | 699 ± 16 | 704 ± 29 | 0.77 | 14.3 | ±28 | 2.0% | 40 (5.6%) |
| CP | FA mean | 670 ± 74 | 694 ± 39 | 0.81 | 34.4 | ±67 | 5.0% | 95 (14.0%) |
| ALIC | FA mean | 550 ± 24 | 563 ± 28 | 0.22 | 24.8 | ±49 | 4.5% | 69 (12.4%) |
| PLIC | FA mean | 651 ± 22 | 625 ± 30 | 0.66 | 22.7 | ±45 | 3.6% | 63 (9.9%) |
| GCC | FA mean | 770 ± 21 | 758 ± 31 | 0.65 | 19.6 | ±38 | 2.6% | 54 (7.1%) |
| SCR | FA mean | 489 ± 28 | 490 ± 36 | 0.79 | 18.8 | ±37 | 3.8% | 52 (10.7%) |
| CING | FA mean | 541 ± 63 | 533 ± 68 | 0.92 | 24.6 | ±48 | 4.6% | 68 (12.7%) |

Abbreviations are listed in Table 1.



NIH-PA Author Manuscript NIH-PA Author Manuscript NIH-PA Author Manuscript